

Inclusive Measurement of the Photon Energy Spectrum in $b \rightarrow s\gamma$ Decays

P. Koppenburg,⁶ K. Abe,⁶ K. Abe,³⁸ T. Abe,⁶ I. Adachi,⁶ H. Aihara,⁴⁰ M. Akatsu,¹⁹ Y. Asano,⁴⁴ V. Aulchenko,¹ T. Aushev,¹⁰ A. M. Bakich,³⁵ Y. Ban,²⁹ A. Bay,¹⁵ U. Bitenc,¹¹ I. Bizjak,¹¹ A. Bondar,¹ A. Bozek,²³ M. Bračko,^{17,11} T. E. Browder,⁵ P. Chang,²² Y. Chao,²² K.-F. Chen,²² B. G. Cheon,³⁴ Y. Choi,³⁴ A. Chuvikov,³⁰ S. Cole,³⁵ M. Danilov,¹⁰ M. Dash,⁴⁶ L. Y. Dong,⁸ A. Drutskoy,¹⁰ S. Eidelman,¹ V. Eiges,¹⁰ Y. Enari,¹⁹ F. Fang,⁵ S. Fratina,¹¹ N. Gabyshev,⁶ A. Garmash,³⁰ T. Gershon,⁶ G. Gokhroo,³⁶ B. Golob,^{16,11} J. Haba,⁶ H. Hayashii,²⁰ M. Hazumi,⁶ T. Higuchi,⁶ L. Hinz,¹⁵ T. Hokuue,¹⁹ Y. Hoshi,³⁸ W.-S. Hou,²² Y. B. Hsiung,^{22,*} T. Iijima,¹⁹ K. Inami,¹⁹ A. Ishikawa,⁶ R. Itoh,⁶ H. Iwasaki,⁶ M. Iwasaki,⁴⁰ J. H. Kang,⁴⁸ J. S. Kang,¹³ N. Katayama,⁶ H. Kawai,² T. Kawasaki,²⁵ H. Kichimi,⁶ H. J. Kim,⁴⁸ J. H. Kim,³⁴ S. K. Kim,³³ T. H. Kim,⁴⁸ S. Korpar,^{17,11} P. Križan,^{16,11} P. Krokovny,¹ S. Kumar,²⁸ A. Kuzmin,¹ Y.-J. Kwon,⁴⁸ J. S. Lange,^{4,31} G. Leder,⁹ S. H. Lee,³³ T. Lesiak,²³ J. Li,³² A. Limosani,¹⁸ S.-W. Lin,²² J. MacNaughton,⁹ G. Majumder,³⁶ F. Mandl,⁹ T. Matsumoto,⁴² Y. Mikami,³⁹ W. Mitaroff,⁹ K. Miyabayashi,²⁰ H. Miyake,²⁷ H. Miyata,²⁵ D. Mohapatra,⁴⁶ G. R. Moloney,¹⁸ T. Mori,⁴¹ T. Nagamine,³⁹ Y. Nagasaka,⁷ T. Nakadaira,⁴⁰ E. Nakano,²⁶ M. Nakao,⁶ Z. Natkaniec,²³ K. Neichi,³⁸ S. Nishida,⁶ O. Nitoh,⁴³ T. Nozaki,⁶ S. Ogawa,³⁷ T. Ohshima,¹⁹ T. Okabe,¹⁹ S. Okuno,¹² S. L. Olsen,⁵ W. Ostrowicz,²³ H. Ozaki,⁶ P. Pakhlov,¹⁰ H. Palka,²³ C. W. Park,¹³ H. Park,¹⁴ N. Parslow,³⁵ L. S. Peak,³⁵ L. E. Piilonen,⁴⁶ F. J. Ronga,⁶ M. Rozanska,²³ H. Sagawa,⁶ S. Saitoh,⁶ Y. Sakai,⁶ T. R. Sarangi,⁴⁵ O. Schneider,¹⁵ C. Schwanda,⁹ A. J. Schwartz,³ S. Semenov,¹⁰ K. Senyo,¹⁹ R. Seuster,⁵ M. E. Sevier,¹⁸ H. Shibuya,³⁷ N. Soni,²⁸ R. Stamen,⁶ S. Stanič,^{44,†} M. Starič,¹¹ T. Sumiyoshi,⁴² S. Suzuki,⁴⁷ O. Tajima,³⁹ F. Takasaki,⁶ N. Tamura,²⁵ M. Tanaka,⁶ G. N. Taylor,¹⁸ T. Tomura,⁴⁰ K. Trabelsi,⁵ T. Tsuboyama,⁶ T. Tsukamoto,⁶ S. Uehara,⁶ T. Uglov,¹⁰ K. Ueno,²² S. Uno,⁶ Y. Ushiroda,⁶ G. Varner,⁵ K. E. Varvell,³⁵ C. C. Wang,²² C. H. Wang,²¹ M. Watanabe,²⁵ B. D. Yabsley,⁴⁶ Y. Yamada,⁶ A. Yamaguchi,³⁹ Y. Yamashita,²⁴ M. Yamauchi,⁶ H. Yanai,²⁵ Heyoung Yang,³³ J. Ying,²⁹ Y. Yusa,³⁹ C. C. Zhang,⁸ Z. P. Zhang,³² T. Ziegler,³⁰ and D. Žontar^{16,11}

(Belle Collaboration)

¹*Budker Institute of Nuclear Physics, Novosibirsk*

²*Chiba University, Chiba*

³*University of Cincinnati, Cincinnati, Ohio 45221*

⁴*University of Frankfurt, Frankfurt*

⁵*University of Hawaii, Honolulu, Hawaii 96822*

⁶*High Energy Accelerator Research Organization (KEK), Tsukuba*

⁷*Hiroshima Institute of Technology, Hiroshima*

⁸*Institute of High Energy Physics, Chinese Academy of Sciences, Beijing*

⁹*Institute of High Energy Physics, Vienna*

¹⁰*Institute for Theoretical and Experimental Physics, Moscow*

¹¹*J. Stefan Institute, Ljubljana*

¹²*Kanagawa University, Yokohama*

¹³*Korea University, Seoul*

¹⁴*Kyungpook National University, Taegu*

¹⁵*Swiss Federal Institute of Technology of Lausanne, EPFL, Lausanne*

¹⁶*University of Ljubljana, Ljubljana*

¹⁷*University of Maribor, Maribor*

¹⁸*University of Melbourne, Victoria*

¹⁹*Nagoya University, Nagoya*

²⁰*Nara Women's University, Nara*

²¹*National United University, Miao Li*

²²*Department of Physics, National Taiwan University, Taipei*

²³*H. Niewodniczanski Institute of Nuclear Physics, Krakow*

²⁴*Nihon Dental College, Niigata*

²⁵*Niigata University, Niigata*

²⁶*Osaka City University, Osaka*

²⁷*Osaka University, Osaka*

²⁸*Panjab University, Chandigarh*

²⁹*Peking University, Beijing*

³⁰*Princeton University, Princeton, New Jersey 08545*

³¹*RIKEN BNL Research Center, Upton, New York 11973*³²*University of Science and Technology of China, Hefei*³³*Seoul National University, Seoul*³⁴*Sungkyunkwan University, Suwon*³⁵*University of Sydney, Sydney, New South Wales*³⁶*Tata Institute of Fundamental Research, Bombay*³⁷*Toho University, Funabashi*³⁸*Tohoku Gakuin University, Tagajo*³⁹*Tohoku University, Sendai*⁴⁰*Department of Physics, University of Tokyo, Tokyo*⁴¹*Tokyo Institute of Technology, Tokyo*⁴²*Tokyo Metropolitan University, Tokyo*⁴³*Tokyo University of Agriculture and Technology, Tokyo*⁴⁴*University of Tsukuba, Tsukuba*⁴⁵*Utkal University, Bhubaneswer*⁴⁶*Virginia Polytechnic Institute and State University, Blacksburg, Virginia 24061*⁴⁷*Yokkaichi University, Yokkaichi*⁴⁸*Yonsei University, Seoul*

(Received 2 March 2004; published 6 August 2004)

We report a fully inclusive measurement of the flavor changing neutral current decay $b \rightarrow s\gamma$ in the energy range $1.8 \text{ GeV} \leq E_\gamma^* \leq 2.8 \text{ GeV}$, covering 95% of the total spectrum. Using 140 fb^{-1} , we obtain $\mathcal{B}(b \rightarrow s\gamma) = (3.55 \pm 0.32_{-0.31}^{+0.30+0.11}) \times 10^{-4}$, where the errors are statistical, systematic, and from theory corrections. We also measure the first and second moments of the photon energy spectrum above 1.8 GeV and obtain $\langle E_\gamma \rangle = 2.292 \pm 0.026 \pm 0.034 \text{ GeV}$ and $\langle E_\gamma^2 \rangle - \langle E_\gamma \rangle^2 = 0.0305 \pm 0.0074 \pm 0.0063 \text{ GeV}^2$, where the errors are statistical and systematic.

DOI: 10.1103/PhysRevLett.93.061803

PACS numbers: 13.20.He, 13.40.Hq, 14.40.Nd, 14.65.Fy

The flavor changing neutral current decay $b \rightarrow s\gamma$ process is of remarkable theoretical interest. Its total branching fraction is very sensitive to physics beyond the standard model as it may be affected by the presence of charged Higgs or supersymmetric particles in the loop. Yet the present theoretical prediction for the branching fraction of $(3.79_{-0.53}^{+0.36}) \times 10^{-4}$ [1,2], and the average experimental value $(3.3 \pm 0.4) \times 10^{-4}$ [3] agree well. This agreement sets a strong constraint on, e.g., models [4] that accommodate the observed difference in CP asymmetries in the $B \rightarrow J/\psi K_S$ and $B \rightarrow \phi K_S$ decays [5]. To obtain stronger constraints on physics beyond the standard model, more precise theoretical predictions and experimental measurements are needed.

On the other hand, the photon energy spectrum is almost insensitive to physics beyond the standard model [6]. At the parton level, the photon is monochromatic with energy $E \approx m_b/2$ in the b quark rest frame. The energy is smeared by the motion of the b quark inside the B meson and gluon emission. A measurement of the moments of this spectrum allows a determination of the b -quark mass and of its motion. This information can then be used to extract the Cabibbo-Kobayashi-Maskawa matrix elements $|V_{cb}|$ and $|V_{ub}|$ from inclusive semileptonic b decays [7,8]. However, a measurement of the low-energy tail of the photon spectrum is important in this context [9].

Belle has previously measured the $b \rightarrow s\gamma$ branching fraction with 5.8 fb^{-1} of data using a semi-inclusive approach. Because we applied an effective cut $E_\gamma >$

2.24 GeV in the B rest frame, the precision of that measurement is limited by theoretical errors due to the extrapolation to the whole energy spectrum. More recently the CLEO collaboration has reported a measurement of the branching fraction and the energy spectrum moments performed in a fully inclusive way [10] for the range $E_\gamma^* > 2.0 \text{ GeV}$ in the center-of-mass frame [11]. Here we present a measurement using a similar approach, but based on a much larger data set allowing a detailed study of the backgrounds. We extend the photon energy range to $E_\gamma^* > 1.8 \text{ GeV}$, covering almost the entire spectrum.

The $b \rightarrow s\gamma$ decay is studied using the Belle detector at the KEKB asymmetric e^+e^- storage ring [12]. The data consist of a sample of 140 fb^{-1} taken at the $Y(4S)$ resonance corresponding to $(152.0_{-0.7}^{+0.6}) \times 10^6$ $B\bar{B}$ pairs. Another 15 fb^{-1} sample has been taken at an energy 60 MeV below the resonance and is used to measure the non- $B\bar{B}$ background. Throughout this Letter, we refer to these data samples as the ON and OFF samples, respectively.

The Belle detector is a large-solid-angle magnetic spectrometer described in detail elsewhere [13]. The main component relevant for this analysis is the electromagnetic calorimeter (ECL) made of 16.2 radiation lengths long CsI(Tl) crystals. The photon energy resolution is about 2% for the energy range relevant in this analysis.

The strategy to extract the signal $b \rightarrow s\gamma$ spectrum is to collect all high-energy photons, vetoing those

originating from π^0 and η decays to two photons. The contribution from continuum $e^+e^- \rightarrow q\bar{q}$ ($q = u, d, s, c$) events is subtracted using the OFF sample. The remaining backgrounds from $B\bar{B}$ events are subtracted using Monte Carlo (MC) distributions scaled by data control samples.

Photon candidates are selected from ECL clusters of 5×5 crystals in the barrel region ($-0.5 \leq \cos\theta \leq 0.84$, where θ is the polar angle with respect to the beam axis). They are required to have an energy E_γ^* larger than 1.5 GeV, and 95% of the energy has to be deposited in the central 3×3 crystal array. We require isolation cuts to veto photons from bremsstrahlung and interaction with matter. The center of the cluster has to be displaced from any other ECL cluster with $E > 20$ MeV by at least 30 cm at the surface of the calorimeter, and from any reconstructed track by 3 cm, or by 50 cm for tracks with a measured momentum above 1 GeV/c. Moreover, the angle between the photon and the highest energy lepton in the event has to be larger than 0.3 radians at the interaction point. We veto candidate photons from π^0 and η decays to two photons by combining them with any other photon. We reject the pair if the likelihood of being a π^0 or η is larger than 0.1 and 0.2, respectively. These likelihoods are determined from MC calculations and are functions of the laboratory energy of the other photon, its polar angle θ and the mass of the two-photon system.

In order to reduce the contribution from continuum events, we use two Fisher discriminants. The first exploits the spherical shape of $B\bar{B}$ events and is built using ten event-shape variables. These variables are calculated using either all tracks and showers in the event or excluding the photon candidate. The event shape variables include Fox-Wolfram moments, thrust, and the angles of the thrust axis with respect to the beam and photon direction. The second discriminant exploits the topology of $b \rightarrow s\gamma$ events and combines three energy flows around the photon axis. These energy flow variables are obtained using all particles, except for the photon candidate, whose direction lies in the three regions defined by $\alpha^* < 30^\circ$, $30^\circ \leq \alpha^* \leq 140^\circ$, $\alpha^* > 140^\circ$, where α^* is the angle to the candidate photon.

To optimize these selection criteria, we use a Monte Carlo simulation [14] containing large samples of $B\bar{B}$, $q\bar{q}$ and signal weighted according to the luminosities of the ON and OFF samples. The signal MC is generated as a weighted sum of $B \rightarrow K^*\gamma$ decays, where K^* is any known spin-1 resonance with strangeness $S = 1$. The relative weights are obtained by fitting the total photon spectrum to a theoretical model [6]. The signal MC is normalized to the average measured branching fraction [3]. To improve the understanding of the photon energy spectrum at low energies, the selection criteria are optimized to maximize the sensitivity to the signal in the energy bin $1.8 \text{ GeV} < E_\gamma^* < 1.9 \text{ GeV}$.

After these selection criteria we observe 1.2×10^6 photon candidates in ON and 1.1×10^5 in OFF data. The spectrum measured in OFF data is scaled by luminosity to the expected number of non- $B\bar{B}$ events in ON data and subtracted. To take into account the effect of the 60 MeV (0.5%) energy difference, the measured OFF energies are scaled by an empirical factor of 1.004 obtained from a MC study. The ON and scaled OFF spectra and their difference are shown in Fig. 1.

We then subtract the backgrounds from B decays from the obtained spectrum. Five background categories are considered: (i) photons from $\pi^0 \rightarrow \gamma\gamma$, which account for more than half of the background in the 1.8–2.8 GeV range; (ii) photons from $\eta \rightarrow \gamma\gamma$; (iii) other real photons (mainly decays of ω , η' , and J/ψ , and bremsstrahlung); (iv) ECL clusters not due to single photons (mainly electrons interacting with matter, K_L^0 and \bar{n}); (v) beam background. For each of these categories we take the predicted background from MC and scale it according to measured yields wherever possible. The inclusive $B \rightarrow \pi^0 X$ and $B \rightarrow \eta X$ spectra are measured in data using pairs of photons with a well-balanced energy and applying the same ON-OFF subtraction procedure. The yields obtained are 5% to 15% larger than MC expectations depending on the photon energy range. Since there is good agreement between MC and data for all features of the GEANT simulation for photons and electrons, we believe that the observed discrepancy between the measured and simulated π^0 spectrum is due to the generator [15]. Beam background is measured using a sample of randomly triggered events and added to the $B\bar{B}$ MC.

For each selection criterion and each background category we determine the E_γ^* -dependent selection efficiency in OFF-subtracted ON data and MC using appropriate

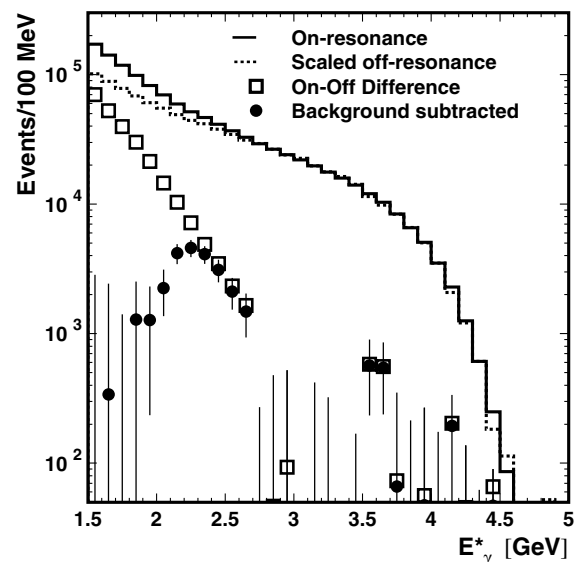


FIG. 1. Photon energy spectra in the $Y(4S)$ frame.

control samples. We then scale the MC background sample according to the ratio of these efficiencies. The efficiencies of the π^0 and η vetoes for non- π^0 , non- η photons are measured in data using one photon from a well reconstructed π^0 applying the veto without using the other photon of the pair. The π^0 veto efficiency is measured using a sample of photons coming from measured π^0 decays. We use partially reconstructed $D^{*+} \rightarrow D^0 \pi^+$, $D^0 \rightarrow K^- \pi^+ \pi^0$ decays where the π^0 is replaced by the candidate photon in the reconstruction. The η veto efficiency for photons from π^0 's and event-shape criteria efficiencies are measured using a π^0 antiveto sample. It is made of photons passing all selection criteria except the π^0 veto, which are combined with another photon in the event to give a π^0 -likelihood larger than 0.75. Other efficiencies are measured using the signal sample.

The ratios of data and MC efficiencies versus E_γ^* are fitted using first or second order polynomials, which are used to scale the background MC. Most are found to be statistically compatible with unity. An exception is the efficiency of the requirement that 95% of the energy be deposited in the central nine cells of the 5×5 cluster, which is found to be poorly modeled by our MC for non-photon backgrounds. We estimate the efficiency for data using a sample of candidate photons in OFF-subtracted ON data after subtracting the known contribution from real photons. This increases the yield of background (iv) by 50%. The yield from the five background categories, after having been properly scaled by the above described procedures, are subtracted from the OFF-subtracted spectrum. The result is shown in Fig. 1.

The spectrum contains $24100 \pm 2140 \pm 1260$ events in the 1.8–2.8 GeV energy range, where the two errors are the statistical error of the OFF-subtracted ON data and of the $B\bar{B}$ background subtractions, and the systematic error related to the data/MC efficiency ratio fits used in the $B\bar{B}$ background scaling. We correct this spectrum for the signal selection efficiency function obtained from signal MC, applying the same data/MC correction factors as for the generic photon background category (iii). The average signal selection efficiency is 23%.

The efficiency-corrected spectrum is shown in Fig. 2. The two error bars for each point show the statistical and the total error, including the systematic error which is correlated among the points. As expected, the spectrum above the end point for decays of B mesons from the $Y(4S)$ at about 3 GeV, is consistent with zero. Integrating this spectrum from 1.8 to 2.8 GeV, we obtain a partial branching fraction of $(3.51 \pm 0.32 \pm 0.29) \times 10^{-4}$.

The sources of systematic error are listed in Table I. They are added in quadrature. The largest sources are the errors of the data/MC efficiency ratio fits (5.9% of the signal yield). For the error related to the choice of the polynomial functions in the data/MC efficiency ratio fits,

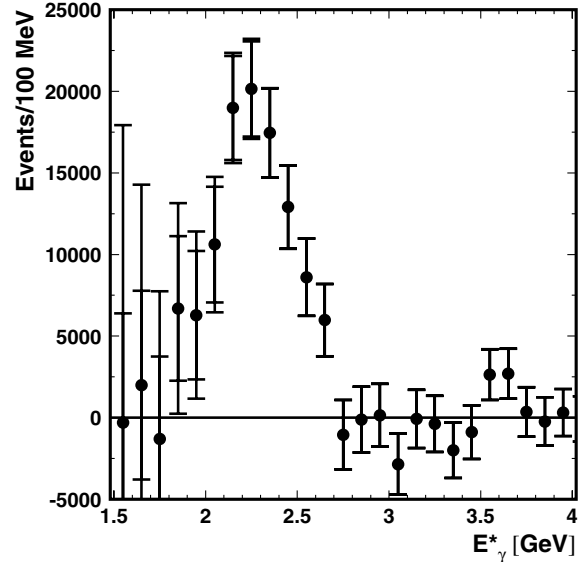


FIG. 2. Efficiency-corrected photon energy spectrum. The two error bars show the statistical and total errors.

we perform the same fit increasing the polynomial order by one. The number of $B\bar{B}$ events is determined from the number of hadronic events in ON and OFF data. The relative luminosities of the two samples are determined from radiative Bhabhas and $e^+e^- \rightarrow \mu^+\mu^-$ events. The errors on the OFF data subtraction are estimated using the result of the fit to the spectrum above the end point. We integrate the resulting function in the 1.8–2.8 GeV range and obtain a yield of $+40 \pm 160$. We add ± 200 (0.8%) to the systematic error. As we do not measure the yields of photons from sources other than π^0 's and η 's in $B\bar{B}$ events, we vary the expected yields of these additional sources by $\pm 20\%$. For the model dependence of signal selection efficiency we use an alternate signal MC that favors high-mass resonances decaying into high-multiplicity final states. Using this MC to correct for the efficiency changes the branching fraction by $\pm 2.5\%$.

TABLE I. Overview of systematic errors.

Source of systematic error	$\times 10^{-4}$
Raw branching fraction	3.51 ± 0.32
Data/MC efficiency ratio fits	± 0.208
Choice of fitting functions	± 0.048
Number of $B\bar{B}$ events	$+0.139$ -0.160
ON-OFF data subtraction	± 0.026
Other $B\bar{B}$ photons	± 0.054
η veto efficiency on η	± 0.008
Signal MC	± 0.089
Photon detection efficiency	± 0.072
Energy leakage	$+0.035$ -0.000
Total error for partial $\mathcal{B}(b \rightarrow q\gamma)$	$+0.282$ -0.291

The error on the photon detection efficiency in the ECL is measured to be 2.3% using radiative Bhabha events. This error also affects the estimation of photons from $B\bar{B}$ and contributes $\pm 2.0\%$ to the systematic error. Because of the low-energy tail in the photon energy measurement, some part of the spectrum may lie below the range of integration. We estimate this fraction to be smaller than 1%. As this value is shape-dependent, we do not correct the measured branching fraction for it but instead add a $(^{+1.0}_{-0.0})\%$ systematic error.

In order to obtain the total $b \rightarrow s\gamma$ branching fraction we apply corrections for the contribution from Cabibbo suppressed $b \rightarrow d\gamma$ decays and for the invisible part of the spectrum below 1.8 GeV. The ratio of the $b \rightarrow s\gamma$ and $b \rightarrow d\gamma$ branching fractions is assumed to be $R_{d/s} = (3.8 \pm 0.6)\%$ [1]. The selection efficiency for $b \rightarrow d\gamma$ is found to be equal to the efficiency for $b \rightarrow s\gamma$ within 10%, which we include in the systematic error. The fraction of the spectrum above 1.8 GeV is assumed to be $R_{1.8} = 0.952^{+0.013}_{-0.029}$ from Gambino and Misiak [2]. As a cross check we also use the value from Kagan and Neubert [6] $R_{1.8} = 0.958^{+0.013}_{-0.029}$, and $R_{1.8} = 0.95 \pm 0.01$ from Bigi and Uraltsev [9]. We combine the errors on $R_{d/s}$, $R_{1.8}$ and the difference between the $R_{1.8}$ values into the theoretical error. With these two corrections, we obtain

$$\mathcal{B}(b \rightarrow s\gamma) = (3.55 \pm 0.32^{+0.30+0.11}_{-0.31-0.07}) \times 10^{-4}$$

for the total $b \rightarrow s\gamma$ branching fraction. This result is in good agreement with theoretical expectations and with previous experimental measurements [10,16].

We also measure the first two moments of the energy spectrum in the B rest frame. We extract the raw moments from the distribution shown in Fig. 2 in the range $1.8 \text{ GeV} \leq E_\gamma^* \leq 2.8 \text{ GeV}$ and correct them for the effect of the boost of the B meson in the $Y(4S)$ frame, for the energy resolution and for the 100 MeV binning. We do not correct the moments for the missing low-energy tail. We obtain the following moments for $E_\gamma^* > 1.8 \text{ GeV}$ (corresponding to $E_\gamma > 1.815 \text{ GeV}$ in the B rest frame):

$$\begin{aligned} \langle E_\gamma \rangle &= 2.292 \pm 0.026 \pm 0.034 \text{ GeV}, \\ \langle E_\gamma^2 \rangle - \langle E_\gamma \rangle^2 &= 0.0305 \pm 0.0074 \pm 0.0063 \text{ GeV}^2, \end{aligned} \quad (1)$$

where the errors are statistical and systematic.

The systematic error contains the errors related to the moments corrections and the error sources already mentioned for the branching fraction extraction. For the first moment the systematic error is dominated by the data/MC efficiency ratio fits ($\pm 0.9\%$) and the shape of the energy resolution ($\pm 1.0\%$). The error on the second moment is dominated by the data/MC efficiency ratio fits ($\pm 17\%$). These results agree within 1σ with the only previous measurement, done by the CLEO

Collaboration [10]. However, it should be noted that the CLEO results are obtained for $E_\gamma^* > 2.0 \text{ GeV}$.

In conclusion, we have measured the branching fraction and photon energy spectrum of $b \rightarrow s\gamma$ in the energy range $1.8 \text{ GeV} \leq E_\gamma^* \leq 2.8 \text{ GeV}$ in a fully inclusive way. For the first time 95% or more of the spectrum is measured, allowing the theoretical uncertainties to be reduced to a very low level. Using 140 fb^{-1} of data taken at the $Y(4S)$ and 15 fb^{-1} taken below the resonance, we obtain $\mathcal{B}(b \rightarrow s\gamma) = (3.55 \pm 0.32^{+0.30+0.11}_{-0.31-0.07}) \times 10^{-4}$, where the errors are statistical, systematic and theoretical, respectively. This result is in good agreement with the latest theoretical calculations [1,2]. We have also measured the moments of the distribution and obtain $\langle E_\gamma \rangle = 2.292 \pm 0.026 \pm 0.034 \text{ GeV}$ and $\langle E_\gamma^2 \rangle - \langle E_\gamma \rangle^2 = 0.0305 \pm 0.0074 \pm 0.0063 \text{ GeV}^2$ for $E_\gamma^* > 1.8 \text{ GeV}$, where the errors are statistical and systematic.

We thank T. Hurth, I. Bigi, A. Kagan, and M. Misiak for helpful discussions and correspondences. We thank the KEKB group for the excellent operation of the accelerator, the KEK Cryogenics group for the efficient operation of the solenoid, and the KEK computer group and the NII for valuable computing and Super-SINET network support. We acknowledge support from MEXT and JSPS (Japan); ARC and DEST (Australia); NSFC (Contract No. 10175071, China); DST (India); the BK21 program of MOEHRD, and the CHEP SRC program of KOSEF (Korea); KBN (Contract No. 2P03B 01324, Poland); MIST (Russia); MESS (Slovenia); NSC and MOE (Taiwan); and DOE (U.S.).

*On leave from Fermi National Accelerator Laboratory, Batavia, IL 60510.

†On leave from Nova Gorica Polytechnic, Nova Gorica.

- [1] T. Hurth, E. Lunghi, and W. Porod, hep-ph/0312260, and references therein.
- [2] P. Gambino and M. Misiak, Nucl. Phys. **B611**, 338 (2001).
- [3] Particle Data Group, K. Hagiwara *et al.*, Phys. Rev. D **66**, 010001 (2002).
- [4] See, for instance, G. Isidori, hep-ph/0401079, and references therein.
- [5] Belle Collaboration, K. Abe *et al.*, Phys. Rev. Lett. **91**, 261602 (2003); Belle Collaboration, K. Abe *et al.*, hep-ex/0308036; see also BABAR Collaboration, B. Aubert *et al.*, hep-ex/0207070; BABAR Collaboration, B. Aubert *et al.*, Phys. Rev. Lett. **89**, 201802 (2002).
- [6] A. Kagan and M. Neubert, Eur. Phys. J. C **7**, 5 (1998).
- [7] M. Neubert, Phys. Rev. D **49**, 4623 (1994); M. Neubert, Phys. Lett. B **513**, 88 (2001), and references therein.
- [8] CLEO Collaboration, D. Cronin-Hennessy *et al.*, Phys. Rev. Lett. **87**, 251808 (2001); CLEO Collaboration, A. Bornheim *et al.*, Phys. Rev. Lett. **88**, 231803 (2002);

- Belle Collaboration, H. Kakuno *et al.*, Phys. Rev. Lett. **92**, 101801 (2004).
- [9] I. Bigi and N. Uraltsev, Int. J. Mod. Phys. A **17**, 4709 (2002).
- [10] CLEO Collaboration, S. Chen *et al.*, Phys. Rev. Lett. **87**, 251807 (2001).
- [11] Throughout this Letter, variables with an asterisk are calculated in the center-of mass frame.
- [12] S. Kurokawa and E. Kikutani, Nucl. Instrum. Methods Phys. Res., Sect. A **499**, 1 (2003), and other papers included in this volume.
- [13] Belle Collaboration, A. Abashian *et al.*, Nucl. Instrum. Methods Phys. Res., Sect. A **479**, 117 (2002).
- [14] Events are generated with the CLEO QQ generator (see <http://www.lns.cornell.edu/public/CLEO/soft/qq>); the detector response is simulated with GEANT, R. Brun *et al.*, GEANT 3.21, CERN Report No. DD/EE/84-1, 1984.
- [15] See also Belle Collaboration, K. Abe *et al.*, Phys. Rev. D **64**, 072001 (2001).
- [16] Belle Collaboration, K. Abe *et al.*, Phys. Lett. B **511**, 151 (2001).